

**The properties of the cardiac cell mathematical model with a
Markovian representation of potassium channel gating
processes under high pacing rate
(Computer simulation study)**

CSD-TR040007

R. Samade, B. Kogan

February 2004

The properties of the cardiac cell mathematical model with a Markovian representation of potassium channel gating processes under high pacing rate (Computer simulation study)

R. Samade, B. Kogan

Computer Science Department, University of California, Los Angeles, California, USA.

1. Abstract

In the last 50 years, many mathematical models of Action Potential (AP) have been formulated and implemented in computer simulation using the gating process description provided by Hodgkin's and Huxley's (H-H) work on the giant squid axon. Beginning with the development of the single-channel clamp measurement technique, a new formulation of the gating processes as a Markov process has been proposed and utilized in the novel AP mathematical models. The Markovian representation provides interdependence of channel gating processes, which is closer to the reality than with the Hodgkin-Huxley formulation, where the gating processes are postulated to be independent. The Markovian representation allows the simulation of structural changes (due to the effects of drugs, toxins, and genetic changes) of channel proteins by implementing the corresponding modifications in channel's kinetics.

Unlike the published investigations of the effects of the Markovian representation on AP generation made predominately for normal and comparatively low pacing rates, here we present the results obtained for high pacing rates, characteristic for heart arrhythmia and fibrillation. These results are related to the case when the Markovian representation of the rapid potassium channels (I_{Kr}) replaces the H-H one in the modified LRd cell model. In the course of computer simulation, we found that single early-after depolarization (EADs) appears in AP of wild-type myocardial cells, namely, of M-type cell with Markovian representation of I_{Kr} channels. For mutated I_{Kr} channel, the single EADs are observed in two cases: in Epi-cell with R56Q mutations and M-cell with T474I mutation. The occurrences of multiple EADs with further transfer to constant membrane potential (cardiac arrest) were observed for M-cell with R56Q mutation of the I_{Kr} channels. Under high pacing rates, the Markovian representation in comparison to the H-H has a tendency to increase the action potential duration and predispose the cell to the appearance of EADs.

2. Introduction

Prior investigations involving mathematical modeling and computer simulation of action potential generation and wave propagation in heart tissue until recently have used the ion channel representation given by the Hodgkin-Huxley (H-H) [1]. With this formulation, several first generation mathematical models [2,3,4] for cardiac action

potential (AP) have been developed. These models being done in the manner of the original Noble model [2] and its further improvements, included data from physiological single-cell clamp experiments.

Recent experiments involving cardiac cell mathematical models have begun to exploit the results of single channel clamp experiments [5], and stimulate an alternative to the H-H formulation used for the voltage and time dependent channels of cardiac and nerve cells [6-10]. This new formulation of the ionic channels, the Markovian formulation, takes into account the fact that the different states probabilities governing the functioning of the ion channel are all interdependent, with the transitions between each of the states controlled by rate kinetics.

The first investigations of the cardiac cell with Markovian representation of the I_{kr} channels involving the effect of mutation have been done for relatively low pacing rates on both Epi and M-cells¹ in [11]. They showed that EADs occur in only one type of mutation, R56Q, and in only one type of cardiac cell, the M-cell, for low pacing rate (2000 ms). In further publication [12], it was found for wild type of Epi-cell that at normal pacing rates the effect of replacement the H-H formulation with Markovian one for I_{kr} channels do not significant changes the characteristics of generated AP. At the same time but under high pacing rates and all other conditions being the same, the transition to Markovian formulation leads to about 60% increase of APD. In this case EADs were observed only after some changes introduced in intracellular Ca^{2+} dynamics (e.g. decrease the $K_{mns(ca)}$ from 1.2 to 1.043 μM).

It remains unclear if for wild type of M-cell with normal Ca^{2+} dynamics the transition to Markovian formulation of I_{kr} channels is enough to cause EADs at high pacing rates. Also, a topic of grate interest involves the effect of I_{kr} channel mutations on appearance of EADs in Epi and M-cells with normal Ca dynamics under high pacing rates. The investigation of these problems for pacing rate characteristic for heart arrhythmias and fibrillation are the subjects of this presentation.

3. Methods

For the cardiac cell simulations, the modified Chudin model for AP [4] was utilized in order to fully take into account the effects of intra-cellular Ca^{2+} dynamics. It represents the Luo-Rudy [13] model with modifications of the intra-cellular Ca^{2+} dynamics. The change in voltage across the membrane of the cell is related to the ionic current by the following general differential equation:

$$\frac{dV}{dt} = -\frac{1}{C_m} (\sum I_s + I_{stimulus}) \quad (1)$$

with V as the membrane potential, $\sum I_s$ as the sum of the ionic currents through the cell membrane, $I_{stimulus}$ as the external applied stimulus current, and C_m as the cell membrane capacity.

In the above expression, the intra-cellular Ca^{2+} dynamics and the currents through the membrane are described by non-linear ordinary differential equations, which are presented in [4]. For Equation (1), appropriate initial conditions as used in [4] are applied

¹ Physiological data presented in [14] show that in normal conditions M-cell has longer APD than Epi-cells

to its numerical solution, with rapid potassium channel initial state probabilities obtained as the steady state values of those probabilities at the AP rest potential. The only modifications made to the initial conditions for the Chudin model are changing the initial values of $[Ca^{2+}]_{i,tot}$ from 18.61 to 21.01 μM and of $[Ca^{2+}]_{jsr,tot}$ from 8.44 to 6.9 mM.

The Hodgkin-Huxley representation according to [15] gives for I_{Kr} :

$$I_{Kr} = G_{Kr} * X_r * R * (V - E_{Kr}), \quad (2)$$

$$E_{Kr} = \frac{R*T}{F} * \ln \frac{[K^+]_0}{[K^+]_i}, [K^+]_0 = 5.4 \text{ mM} \quad (3)$$

Where: G_{Kr} is the maximum conductance of the I_{Kr} channels, V is the membrane potential, and E_{Kr} is the reverse potential. The variables that are contained within Eq. (2) are in turn expressed as:

$$G_{Kr} = 0.02614 * \sqrt{\frac{[K^+]_0}{5.4}}; \quad R = \frac{1}{1 + e^{\frac{V+9}{22.4}}}. \quad (4)$$

$$\frac{dX_r}{dt} = \frac{X_{r(\infty)} - X_r}{\tau_{X_r}(V)}; \quad \text{with initial condition } X_{r(0)} = 0.00017; \quad (5)$$

$$X_{r(\infty)} = \frac{1}{1 + e^{\frac{V+21.5}{7.5}}}; \quad \tau_{X_r} = \frac{1}{\frac{(0.00138)(V_1)}{(1 - e^{-(0.123*V_1)})} + \frac{(0.00061)(V_2)}{(e^{(0.145*V_2)} - 1)}}$$

where $V_1 = V + 14.2$ and $V_2 = V + 38.9$.

In order to use ventricular AP model [4] with H-H representation for both Epi and M-cells types, we used the values of ratio G_{Ks}/G_{Kr} obtained in [16] for each of the cell type. The cardiac cell model then utilized a minor change in the G_{kr} value according to given ratio. Namely, for the simulated Epi-Cardial cell, this $G_{ks}:G_{kr}$ ratio is $G_{ks} = 15 * G_{kr}$ and for the M-Cell, the relation is $G_{ks} = 7 * G_{kr}$. After allowing a simulated run time of ~ 10 s, each myocyte model with different representations of I_{kr} channels was paced at high (BCL = 180 ms) and low (BCL = 750 ms) pacing rates outputting during the run time the APs., I_{Kr} , and the open probability of the I_{kr} channel.

In addition to examining the effects of different myocyte type properties in the frame of the same channel formulation, we studied the effects of different formulation of the I_{Kr} channel for the same myocyte type as well. This was accomplished by replacing in the cell model [4] the Hodgkin-Huxley formulation by Markovian using the same pacing rates.

The Markovian representation of the rapid potassium channel was used according to Clancy and Rudy [11] (for details see Appendix A and B)..

The expression for the Current I_{Kr} for this case takes the form:

$$I_{Kr} = G_{Kr} P(O)(V - E_K) \quad (6)$$

Here $P(O)$ is a probability that single I_{Kr} channel is in the open state obtained as solution of corresponding channel state probabilities equations(see Appendix B),

$G_{Kr} = 0.0135([K^+]_o)^{0.59}$ is the maximum value of all membrane I_{Kr} channels conductance with $[K^+]_o=4.5\text{mM}$, E_{Kr} is the reverse potential expressed by (3).

All mathematical model equations including both Markovian and H-H models of I_{Kr} channels were implemented on a sequential PC computer and run with periodical application (BCL=180ms) of the above-threshold stimuli. The Euler's explicit numerical method was used with variable time step (from 0.005 to 0,1ms) depending on the speed of the corresponding fast variables. To improve accuracy of the solution the equation for sodium gate variable, m , is solved using so called Hybrid method [17] with constant time step $\Delta t = 0.005\text{ms}$. To shorten the time of computations the given functions of membrane potential were preliminary tabulated. Thus, the basic arithmetic operations are replaced by accessing the indexed elements in an array, which requires less computational time.

4. Simulation Results and Discussion

All computer simulation results are divided on two parts: one related to the wild type Epi and M-cell and other to the same cells but with mutated I_{Kr} channels

A summary of the results for the first part is presented in Table 1. These data affirm the well-known fact that M-cell have longer AP then Epi-cell and that the transfer from H-H representation to Markovian increases the APD for both cell types only at high pacing rates. The data in this table were measured for two APs: once after 450 ms from the beginning of stimulation and second time after 630 ms. shown in Fig.1. These allows to avoid the transient period of establishing the AP and the effect of the Ca^{2+} spontaneous release from GSR and thus show what is the effect of different I_{Kr} channel representations. For all experiments the cell model remaining at normal $K_{\text{mns}(\text{Ca})} = 1.2 \mu\text{M}$. , $K_{\text{mns}(\text{Ca})}$ is a coefficient, which determines the sensitivity of the non-selective calcium activated membrane current to $[\text{Ca}^{2+}]_i$. The appearance of EADs is a result of temporal misbalance of total inward and outward membrane currents during repolarization phase of an AP when total outward current is prevailed. The effects of type of the cardiac cell, pacing rates and membrane currents dependent of Ca_i dynamics, representation of I_{Kr} channels in the cell model on appearance of EADs are found after stopping the stimulation as it is shown in Fig. 2. Here, all the results are obtained for wild type of cells under high pacing rate (BCL=180ms). Arrows indicate the moment of last stimulation far away from the beginning (to guarantee the presence of Ca^{2+} accumulation and spontaneous release), which is chosen to concise with the moment of Ca^{2+} spontaneous release from GSR. From Fig. 2 follows that transfer from H-H to Markovian representation for Epi-cell leads to the prolongation of APD, while for M-cell to the appearance of EAD. This occurs due to the facts that Markovian representation of I_{Kr} channel gives smaller value of overage channel open probability than H-H in case of high pacing rates (see Table 1.) and that M-cell in normal condition has longer APD than Epi-cell (see [16]) on account of decreased G_{Ks} .

This makes the cardiac M-Cell more susceptible to the appearance of EAD. Indeed, EADs appear only in M-Cells with the Markovian representation under normal $K_{\text{mns}(\text{Ca})}$ and at high pacing rates.

For simulations of the mutant M-Cells and Epi-Cells, we have chosen the T474I and R56Q mutations of I_{Kr} channel according to Clancy and Rudy [11] but at higher pacing rates (BCL =180 ms for Epi-cell and 240 for M-cell). The decrease of pacing rate to BCL=240ms for M-cell with its natural prolongation of APD (Fig. 3C,D) was done to provide the catching of a rhythm some time before the Ca^{2+} spontaneous release occurs. All the computer simulation results are presented in Fig. 3 and Fig. 4. Fig.3 and Table 2 underline that considered mutations in I_{Kr} channels of Epi and M-cell lead to further increase of APD in conditions when Ca^{2+} spontaneous release is absent. As previously, in Fig. 4 the arrows show the moment of stopping the stimulations.

After stopping the stimulations, the results of T474I mutation in I_{Kr} channel of Epi-cell (Fig. 4(A)) is only an elongation of the APD in comparison to that for wild-type Epi-cell (Fig. 2D). There is no presence of EAD activity. However, the presence of a single EAD can be seen, due to the effects of R56Q type mutation in Epi-cell shown in Fig. 4(B). A comparison of the effect of different types of mutation in I_{Kr} channel of the M-Cell's presented in Fig. 4(C) and Fig. 4(D) shows that T474I type of mutation give single EAD and cardiac arrest after multiple EADs for R56Q type mutation.

The presented results show that the mutations in I_{Kr} channels have a profound effect on the appearance of EADs, for both cell types not only in the case of long period of stimulation [11], but also under high pacing rates.

High pacing rates facilitate the appearance of EADs causing the temporal increase of total Ca_i dependent inward membrane currents and decreasing the open probability of I_{Kr} channels (for Markovian representation), which in turn decreases the rapid outward potassium current. These effects are strongly manifested in M-cell with its natural lowering of slow potassium current and are amplified in the presence of I_{Kr} channels mutations.

The presented results have qualitative character. They are obtained using semi phenomenological mathematical model, in which calcium induced, calcium release processes as well as gating processes are formulated using particular experimental data.

6. Conclusion

The computer simulations of cardiac Epi and M-cell AP mathematical models under high pacing rates show that EADs can be observed in the following cases:

1. Single EADs for wild type cardiac M-cell with Markovian representation of I_{Kr} channels and for M-cell with T474I mutation of I_{Kr} channels.
2. Single EADs for Epi-cell with R56Q mutation of I_{Kr} channels
3. Multiple EADs with transfer to cardiac arrest for M-cell with R56Q mutation of I_{Kr} channels

Acknowledgements:

This study was supported partly by NIH Grant SCOR in Sudden Cardiac Death P50 HL52319. We thank Drs James Weiss and Eugene Chudin for useful discussion and comments.

7. References

- [1] Hodgkin, A.L., Huxley, A.F., 1952. A Quantitative Description of Membrane Currents and its Applications to conduction and Excitation in Nerve. *J. Physiol.*, 117, pp 500-544.

- [2] Noble, D. 1962. A Modification of the Hodgkin-Huxley Equations Applicable to Purkinje Fiber Action and Pace-Maker Potentials. *J. Physiol.*, 160, 317-352.
- [3] Chudin, E., Garfinkel, E., Weiss, J., & Kogan, B. 1998. Wave Propagation In Cardiac Tissue and effects of Intracellular Calcium Dynamics. *Progress in Biophysics & Molecular Biology*, Vol 69, No 2/3, pp 225-236.
- [4] Chudin, E., Goldhaber, J., Garfinkel, A., Weiss, J., & Kogan, B. 1999. Intracellular Ca^{2+} dynamics and the stability of Ventricular Tachycardia. *Biophys. J.*, 77, 2930-2941.
- [5] Sakmann, B. & Neher, E., 1983. *Single Channel Recording*. Plenum Press
- [6] Hille, B. *Ionic Channels of Excitable Membrane*. 1992. Sinauer Assoc. Inc. Second Edition.
- [7] Armstrong, C. & Bezanilla, F. 1997. Inactivation of the sodium current. I, II *J. Gen. Physiol.*, 70:549-590.
- [8] Vandenberg, C. & Bezanilla, F. 1991. Sodium channel gating model of the giant squid axon. *Biophys. J.*, V 60, pp 1511-1533.
- [9] Almers, W., 1978. Gating Currents and Charge Movements in Excitable Membrane. *Rev. Physiol. Biochem. Pharmacol.* 82: 96-190.
- [10] Kuo, C. & Bean, B., 1994. Na^+ Channels Must Deactivate to Recover from Inactivation. *Neuron*, 12: 819-829.
- [11] Clancy, C & Rudy, Y., 2001. Cellular consequences of HERG mutations in Long QT syndrome: precursor of sudden cardiac death. *Cardiovasc. Res.* 50, 301-313.
- [12] Kogan, B., Better, J., & Zlochistyy, I. 2002. The cardiac cell model at normal and high pacing rates with Markovian representations of gating processes. *Simulations in Biomedicine V*, pp 15-24.
- [13] Luo, C. H., and Rudy, Y. 1994. A dynamic model of the cardiac ventricular action potential. I. Simulations of ionic currents and concentration changes. *Circ. Res.* 74: 1071-1096
- [14] Antzelevitch, C., Sicouri, S., Lukas, A., Nesterenko, V., Liu, D., Di Diego, J. 1995. Regional differences in the electrophysiology of ventricular cells: Physiological and Clinical Implications. *Cardiac Electrophys.: From Bench to Bedside*. 228-245.
- [15] Zeng, J., Laurita, K.R., Rosenbaum, D.S., & Rudy, Y., 1995. Two components of the delayed rectifier K^+ current in ventricular myocytes of the guinea pig type. *Circ. Res.* 77, 140-152.
- [16] Viswanathan, P.C., Shaw, R.M., & Rudy, Y. 1999. Effects of I_{kr} and I_{ks} heterogeneity on action potential duration and its rate dependence. *Circulation* 99: 2466-2474.
- [17] Chudin, E. *Instability of Cardiac Excitation Wave Propagation and Intracellular Calcium Dynamics*. 1999. Dissertation for PhD degree in Biomathematics, UCLA
- [18] Kogan, B. Huffaker, R., Lamp, S., Weiss, J. 2003. EAD and Pulse Circulation in a 1D Ring-Shaped Cardiac Tissue with Pronounced Effect of Ca^{2+} Dynamics (Computer Simulation Study). Unpublished.

Characteristics for wild type Epi and M-Cells with Hodgkin-Huxley and Markovian Representations of the I_{Kr} channel at various pacing rates (BCL).					
	Characteristics	M-Cell, BCL 750 ms	Epi-Cell, BCL 750 ms	M-Cell, BCL 180 ms	Epi-Cell, BCL 180ms
Hodgkin-Huxley Representation	APD ₉₀ @ T _s = 450 ms	182 ms	148 ms	143 ms	119 ms
	APD ₉₀ @ T _s = 630 ms	182 ms	148 ms	136 ms	114 ms
	[APD ₉₀] _{Average}	182 ms	148 ms	140 ms	117 ms
	(I _{Kr}) _{max} @ T _s = 450 ms	1.027 $\mu\text{A}/\mu\text{F}$	1.046 $\mu\text{A}/\mu\text{F}$	1.018 $\mu\text{A}/\mu\text{F}$	1.018 $\mu\text{A}/\mu\text{F}$
	(I _{Kr}) _{max} @ T _s = 630 ms	1.027 $\mu\text{A}/\mu\text{F}$	1.046 $\mu\text{A}/\mu\text{F}$	1.009 $\mu\text{A}/\mu\text{F}$	1.009 $\mu\text{A}/\mu\text{F}$
	[(I _{Kr}) _{max}] _{Average}	1.027 $\mu\text{A}/\mu\text{F}$	1.046 $\mu\text{A}/\mu\text{F}$	1.014 $\mu\text{A}/\mu\text{F}$	1.014 $\mu\text{A}/\mu\text{F}$
	P(O) _{max} @ T _s = 450 ms	0.742	0.767	0.717	0.733
	P(O) _{max} @ T _s = 630 ms	0.742	0.767	0.7	0.725
	[P(O) _{max}] _{Average}	0.742	0.767	0.709	0.729
	Appearance of EAD	No	No	No	No
	Markovian Representation	APD ₉₀ @ T _s = 450 ms	183 ms	146 ms	164 ms
APD ₉₀ @ T _s = 630 ms		183 ms	146 ms	171 ms	145ms
[APD ₉₀] _{Average}		183 ms	146 ms	168 ms	147.5 ms
(I _{Kr}) _{max} @ T _s = 450 ms		0.852 $\mu\text{A}/\mu\text{F}$	0.867 $\mu\text{A}/\mu\text{F}$	0.842 $\mu\text{A}/\mu\text{F}$	0.858 $\mu\text{A}/\mu\text{F}$
(I _{Kr}) _{max} @ T _s = 630 ms		0.852 $\mu\text{A}/\mu\text{F}$	0.867 $\mu\text{A}/\mu\text{F}$	0.842 $\mu\text{A}/\mu\text{F}$	0.850 $\mu\text{A}/\mu\text{F}$
[(I _{Kr}) _{max}] _{Average}		0.852 $\mu\text{A}/\mu\text{F}$	0.867 $\mu\text{A}/\mu\text{F}$	0.842 $\mu\text{A}/\mu\text{F}$	0.854 $\mu\text{A}/\mu\text{F}$
P(O) _{max} @ T _s = 450 ms		0.484	0.525	0.433	0.475
P(O) _{max} @ T _s = 630 ms		0.484	0.525	0.417	0.458
[P(O) _{max}] _{Average}		0.484	0.525	0.425	0.467
Appearance of EAD		No	No	Yes	No

Table 1.

Characteristics for wild type Epi and M-Cells with Hodgkin-Huxley (H-H) and Markovian Representations of the I_{Kr} channel at various pacing rates (BCL). In the above table, T_s is the time from the beginning of stimulation when the characteristic of interest is measured, (I_{Kr})_{max} is the maximum value of the rapid potassium channel current, and P(O)_{max} is the maximum value of the I_{Kr} channel's probability of being open. The appearance of early afterdepolarization (EAD) was observed after stopping stimulations (see Fig. 2).

Characteristics for Epi and M-Cells with T474I and R56Q mutations of the I_{Kr} channel at various pacing rates (BCL).					
Markovian Representation	Characteristics	Epi-Cell		M-Cell	
		T474I, BCL 180 ms	R56Q, BCL 180 ms	T474I, BCL 240 ms	R56Q, BCL 240 ms
	$APD_{90} @ T_s = T_s^1$	154.6 ms	161 ms	201.1 ms	218.9 ms
	$APD_{90} @ T_s = T_s^2$	147 ms	150.8 ms	201.6 ms	225.3 ms
	$[APD_{90}]_{Average}$	150.8 ms	155.9 ms	201.4 ms	222.1 ms
	$P(O)_{max} @ T_s = T_s^1$	0.529	0.227	0.517	0.215
	$P(O)_{max} @ T_s = T_s^2$	0.520	0.217	0.506	0.215
	$[P(O)_{max}]_{Average}$	0.525	0.222	0.512	0.215

Table 2.

Characteristics for Epi and M-Cells with T474I and R56Q mutations of the I_{Kr} channel at various pacing rates (BCL). In the above table, T_s^1 and T_s^2 are the times from the beginning of stimulation when the characteristic of interest is measured and $P(O)_{max}$ is the maximum value of the I_{Kr} channel's probability of being open. For the above cases, T_s^1 and T_s^2 correspond to 450 and 630 ms respectively for the T474I and R56Q Epi-Cells, 540 and 780 ms respectively for the T474I M-Cell, and 490 and 730 ms respectively for the R56Q M-Cell.

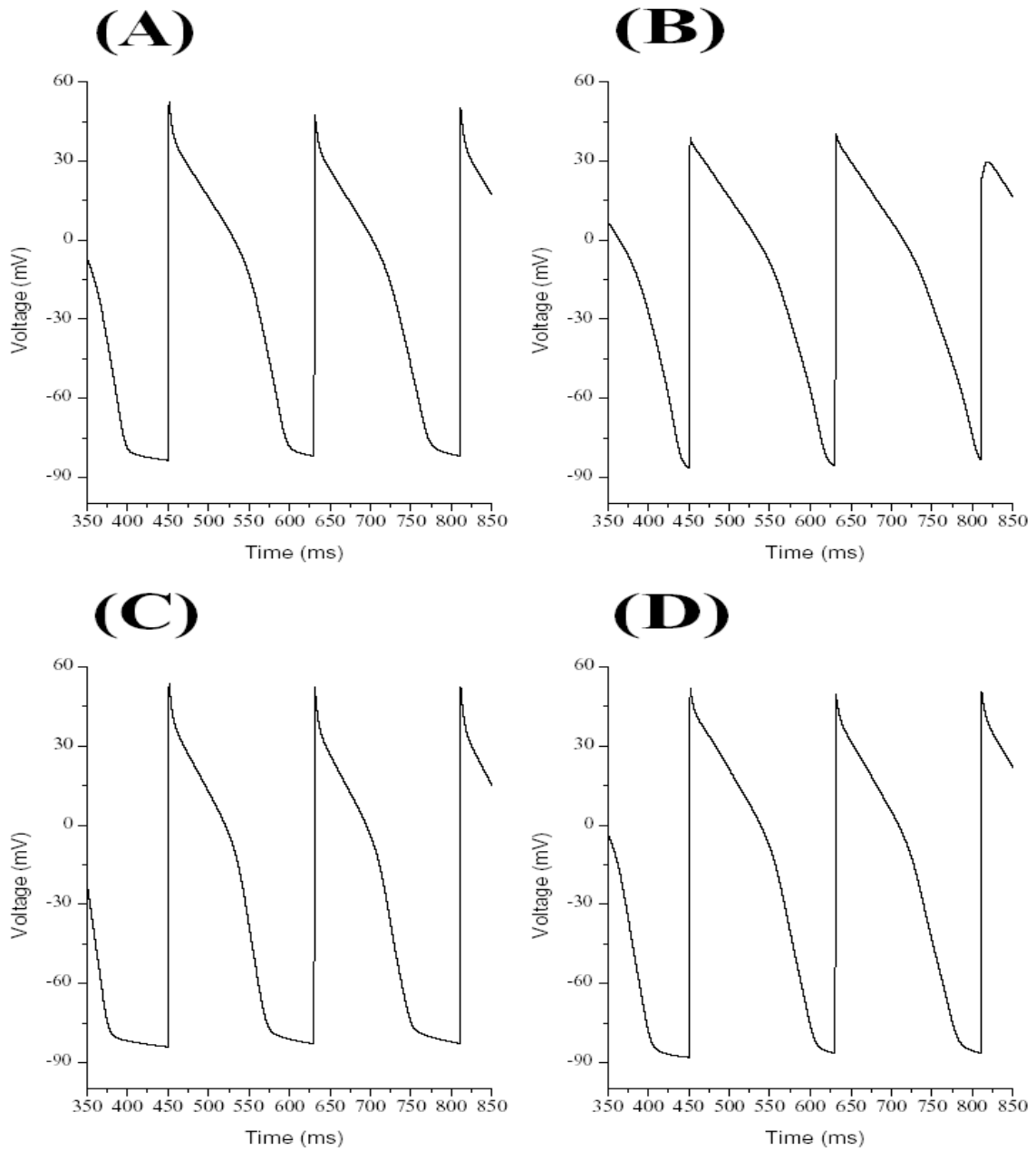


Figure 1.

The presented AP's are paced with BCL = 180 ms. (A) For the wild type Hodgkin-Huxley (H-H) M-Cell, (B) for the wild type Markovian M-Cell, (C) for the wild type H-H Epi-Cell, and (D) for the wild type Markovian Epi-Cell. These AP's are chosen at the beginning of the simulation, in the time interval when spontaneous Ca^{2+} release is not apparent.

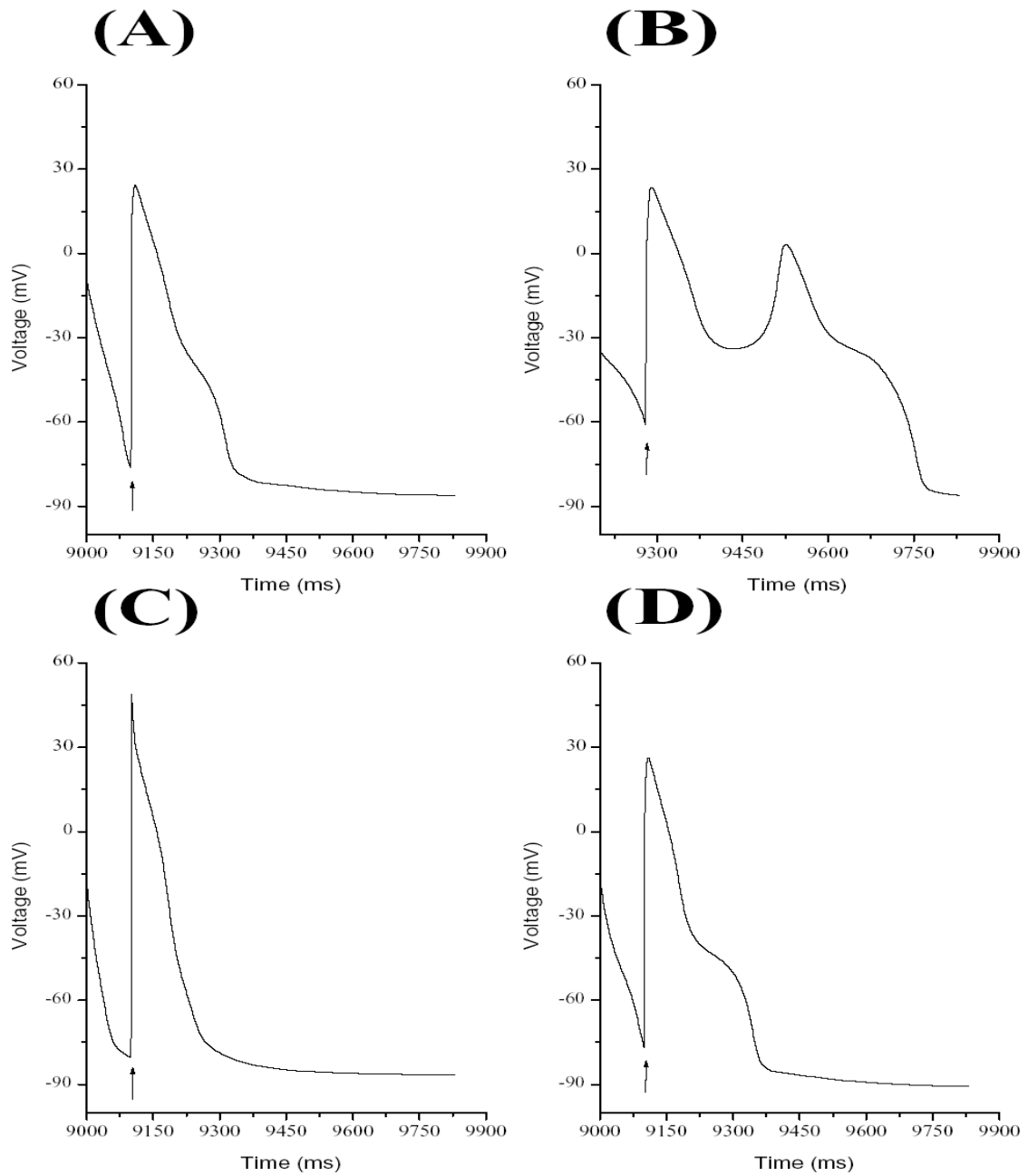


Figure 2.

The presented AP's are paced with BCL = 180 ms. (A) For the wild type Hodgkin-Huxley (H-H) M-Cell, (B) for the wild type Markovian M-Cell, (C) for the wild type H-H Epi-Cell, and (D) for the wild type Markovian Epi-Cell. These AP's are chosen at the time the last stimulus is applied, which coincides with a peak of spontaneous Ca^{2+} release, therefore creating favorable conditions for the appearance of EADs.

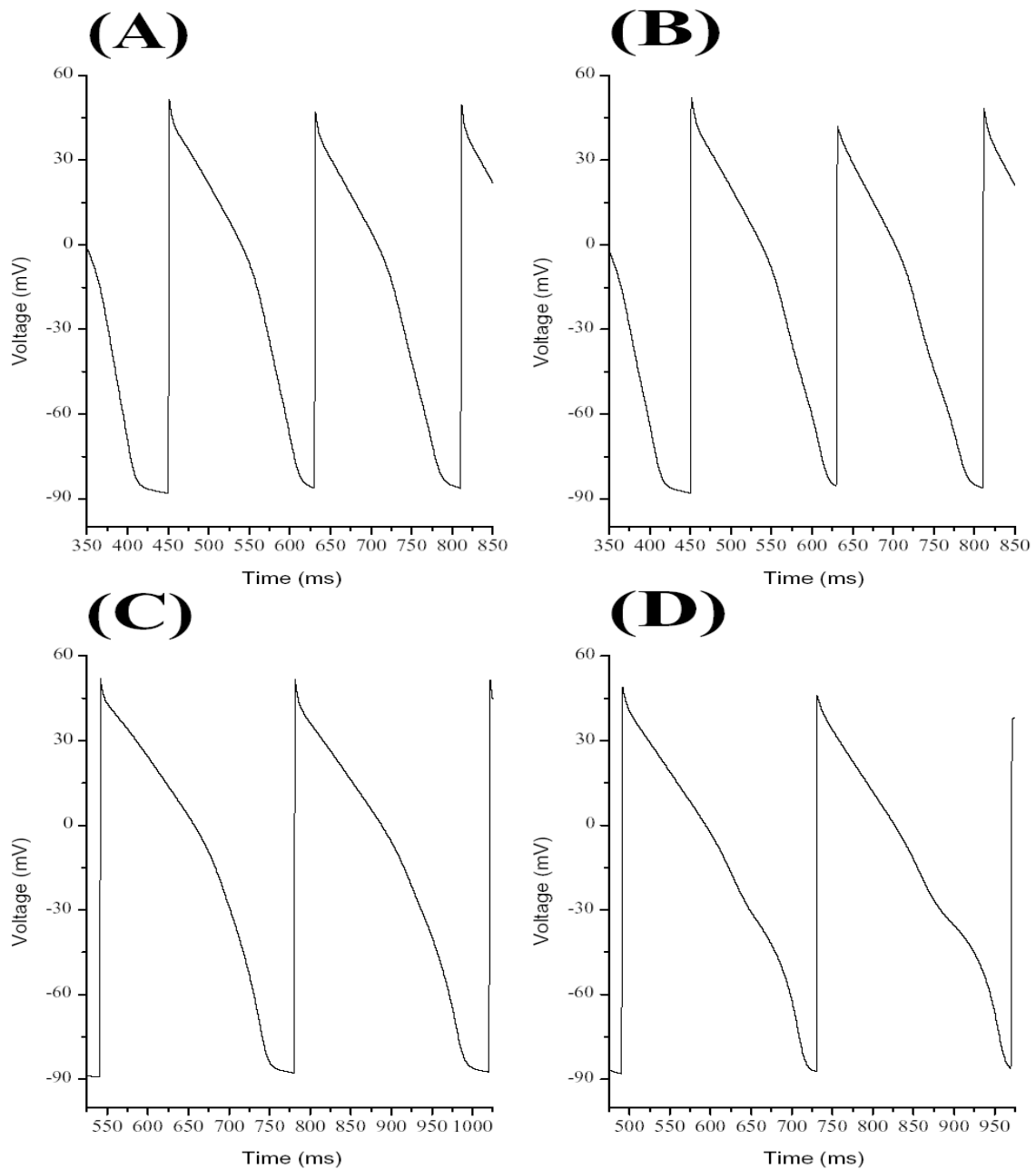


Figure 3.
 The presented AP's are paced with BCL = 180 ms. (A) For the T474I Mutant Markovian Epi-Cell and (B) for the R56Q Mutant Markovian Epi-Cell. The presented AP's paced with BCL = 240 ms are (C) for the T474I Mutant Markovian M-Cell and (D) for the R56Q Mutant Markovian M-Cell. These AP's are chosen at the beginning of the simulation, in the time interval when spontaneous Ca^{2+} release is not apparent.

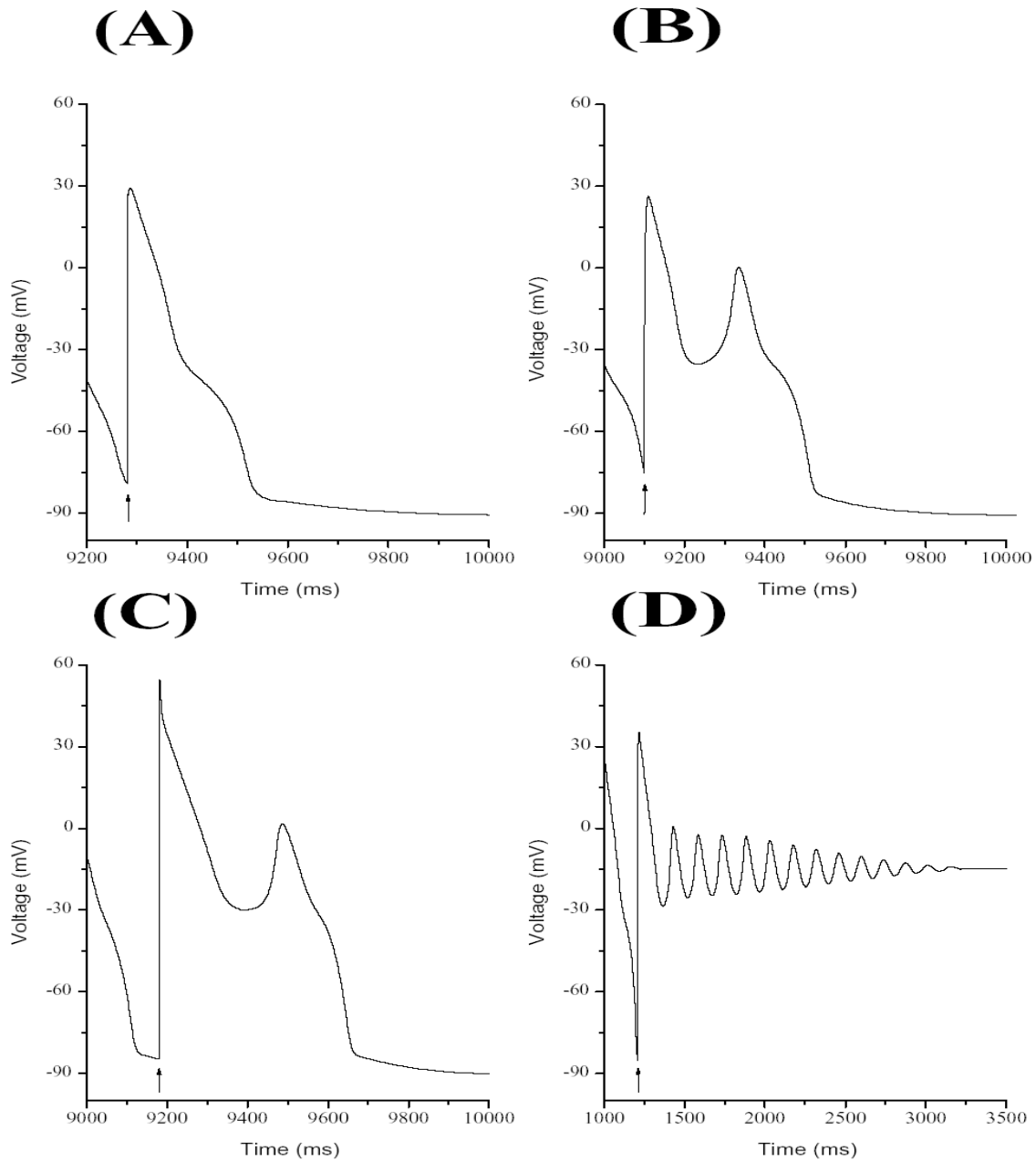


Figure 4.

The presented AP's are paced with BCL = 180 ms (A) for the T474I Mutant Markovian Epi-Cell and (B) for the R56Q Mutant Markovian Epi-Cell. The AP's paced with BCL = 240 ms are (C) for the T474I Mutant Markovian M-Cell and (D) for the R56Q Mutant Markovian M-Cell. These AP's are chosen at the time the last stimulus is applied, which coincides with a peak of spontaneous Ca^{2+} release, therefore creating favorable conditions for the appearance of EADs.

Appendix (A)

Description of the Clancy and Rudy Markovian Model of the Rapid Potassium Channel I_{Kr} :

The I_{Kr} channel proposed by Clancy and Rudy [11] is represented by a total of five possible probability states: the three closed probability states C_1 , C_2 , C_3 ; an open probability state, O ; and an inactivation probability state, I . In terms of independent variables, most of the transition rates are solely voltage dependent, with the exception of the transitions between the C_2 and C_1 closed probability states being voltage independent and the transitions between O and I being dependent on $[K^+]_o$ in addition to voltage. Treating these states as dependent variables, they can be described from the below diagram as a system of five interconnected and linear differential equations, with the transition rates being either constant or dependent on voltage and possibly $[K^+]_o$.

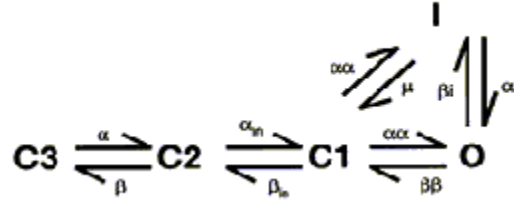


Figure 1A: Block diagram for Markovian model of cardiac cell rapid potassium channel (please see Appendix (B) for the equations giving the model's mathematical description).

Thus, with the Markovian representation, the expression of the current I_{Kr} will be:

$$I_{Kr} = G_{Kr} * P(O) * (V_m - E_K), \quad (9)$$

where $P(O)$ is the open probability of a channel, G_{Kr} is the maximum value of membrane K_r channels conductance, E_K is the reverse potential, and V_m is the membrane potential. In this modified representation, G_{Kr} is altered to become

$$G_{Kr} = 0.0135 * ([K^+]_o)^{0.59}, \quad (10)$$

with $[K^+]_o = 4.5$ mM and the expression for E_K remaining un-altered from the Hodgkin-Huxley representation. As for the open probability $P(O)$, its solution is obtained from solving the system of five equations for channel state probabilities (given below).

Linear Ordinary Differential Equations that Describe the Probability States (C_3 , C_2 , C_1 , O , and I) of the Markovian Cell Model:

$$\frac{dC_3}{dt} = \beta * C_2 - \alpha * C_3$$

$$\frac{dC_2}{dt} = \alpha * C_3 + \beta_{in} * C_1 - (\beta + \alpha_{in}) * C_2$$

$$\frac{dC_1}{dt} = \alpha_{in} * C_2 + \mu * I + \beta\beta * O - (\beta_{in} + 2\alpha\alpha) * C_1$$

$$\frac{dO}{dt} = \alpha\alpha * C_1 + \alpha i * I - (\beta\beta + \beta i) * O$$

$$\frac{dI}{dt} = \alpha\alpha * C_1 + \beta i * O - (\mu + \alpha i) * I$$

$$\frac{dC_3}{dt} + \frac{dC_2}{dt} + \frac{dC_1}{dt} + \frac{dO}{dt} + \frac{dI}{dt} = 0$$

Rate Constants for the Wild-Type Markovian Ventricular Myocyte:

$$\underline{C1 \rightarrow O \text{ or } C1 \rightarrow I}: \alpha\alpha = 65.5 * 10^{-3} * e^{((0.05547153) * (v-36))}$$

$$\underline{C2 \rightarrow C1}: \alpha_{in} = 2.172$$

$$\underline{C3 \rightarrow C2}: \alpha = 55.5 * 10^{-3} * e^{((0.05547153) * (v-12))}$$

$$\underline{C2 \rightarrow C3}: \beta = 2.357 * 10^{-3} * e^{((-0.036588) * (v))}$$

$$\underline{C1 \rightarrow C2}: \beta_{in} = 1.077$$

$$\underline{O \rightarrow C1}: \beta\beta = 2.9357 * 10^{-3} * e^{((-0.02158) * (v))}$$

$$\underline{I \rightarrow O}: \alpha i = 0.439 * \frac{4.5}{[K^+]_{out}} * e^{((-0.02352) * (v+25))}$$

$$\underline{O \rightarrow I}: \beta i = 0.656 * \frac{4.5^{0.3}}{[K^+]_{out}^{0.3}} * e^{((0.000942) * (v))}$$

$$\underline{I \rightarrow C1}: \mu = (\alpha i * \beta\beta * \alpha\alpha) / (\alpha\alpha * \beta i)$$

Appendix (B)

Changes made to the modified cardiac cell model (Chudin model) to simulate the HERG mutations as presented by Clancy and Rudy:

Simulation of T474I Mutation:

Changing the $\alpha\alpha$ rate constant of the $C1 \rightarrow O$ state transition

$$\text{From: } \alpha\alpha = 65.5 * 10^{-3} * e^{((0.05547153) * (v-36))}$$

$$\text{To: } \alpha = 65.5 * 10^{-3} * e^{((0.05547153) * (v+25))}$$

Changing the α rate constant of the C3→C2 state transition

$$\text{From: } \alpha = 55.5 * 10^{-3} * e^{((0.05547153) * (v-12))}$$

$$\text{To: } \alpha = 55.5 * 10^{-3} * e^{((0.05547153) * (v+6))}$$

Changing the value of Gkr

$$\text{From: } G_{Kr} = 0.0135 * ([K^+]_0)^{0.59}$$

$$\text{To: } G_{Kr} = 0.65 * 0.0135 * ([K^+]_0)^{0.59} \text{ (Reduction of 35\%)}$$

Simulation of R56Q Mutation:

Changing the β rate constant of the C2→C3 state transition

$$\text{From: } \beta = 2.357 * 10^{-3} * e^{((-0.036588) * (v))}$$

$$\text{To: } \beta = 10.5 * 2.357 * 10^{-3} * e^{((-0.036588) * (v))}$$

Changing the $\beta\beta$ rate constant of the O→C1 state transition

$$\text{From: } \beta\beta = 2.9357 * 10^{-3} * e^{((-0.02158) * (v))}$$

$$\text{To: } \beta\beta = 6.3 * 2.9357 * 10^{-3} * e^{((-0.02158) * (v))}$$